COMET 81P/WILD 2: THE UPDATED STARDUST COMA DUST FLUENCE MEASUREMENT FOR SMALLER (SUB 10-MICROMETRE) PARTICLES. M. C. Price[1], A. T. Kearsley[2], M. J. Burchell[1], F. Hörz[3] and M. J. Cole[1]. [1]School of Physical Sciences, University of Kent, Canterbury, CT2 7NH, UK (mcp2@star.kent.ac.uk), [2]IARC, Dept. of Mineralogy, The Natural History Museum, London, SW7 5BD, UK, [3]LZ Technology/ESCG, NASA Johnson Space Centre, Houston, TX, USA.

Introduction: Micrometre and smaller scale dust within cometary comae can be observed by telescopic remote sensing spectroscopy [1] and the particle size and abundance can be measured by in situ spacecraft impact detectors [2]. Initial interpretation of the samples returned from comet 81P/Wild 2 by the Stardust spacecraft [3] appears to show that very fine dust contributes not only a small fraction of the solid mass, but is also relatively sparse [4], with a low negative power function describing grain size distribution, contrasting with an apparent abundance indicated by the on-board Dust Flux Monitor Instrument (DFMI) [5] operational during the encounter. For particles above 10 μm diameter there is good correspondence between results from the DFMI and the particle size inferred from experimental calibration [6] of measured aerogel track and aluminium foil crater dimensions (as seen in Figure 4 of [4]). However, divergence between data-sets becomes apparent at smaller sizes, especially submicrometre, where the returned sample data are based upon location and measurement of tiny craters found by electron microscopy of Al foils. Here effects of detection efficiency 'tail-off' at each search magnification can be seen in the down-scale 'flattening' of each scale component, but are reliably compensated by sensible extrapolation between segments. There is also no evidence of malfunction in the operation of DFMI during passage through the coma (S. Green, personal comm.), so can the two data sets be reconciled?

Recent work [7] suggests that the efficiency of Al foil crater excavation by very small particles may be lower than for larger grains, implying that a new calibration is required for this part of the size distribution. The calibrations of [4] were based upon light gas gun (LGG) shots of sodalime glass particles between ~10 and 100 μm, using projectiles with monodispersive size distributions. The data gave a good statistical fit to a line with a constant gradient across the measured sizes, which, within the errors, extrapolated close to the origin, albeit with relatively large error bars. At that time this uncertainty could not be resolved due to a lack of suitable projectiles of <10 μm diameter. This was particularly unfortunate as subsequent analysis of the returned Stardust Al foils indicated that the majority of impact craters were made by particles smaller than 10 μm. The availability of large numbers of monodisperse micrometre and smaller scale projectiles of known density, and their successful acceleration in LGG shots have proven elusive goals, only recently resolved. In this paper we describe new calibration experiments, their preliminary results and the implications for interpretation of particle sizes responsible for the smallest Stardust craters.

Experimental methodology: Shots were performed using the two-stage LGG at the University of Kent [8]. Projectile materials were monodispersive silica spheres commercially available from Whitehouse Scientific (UK) and Micromod (Germany). SEM/EDX imaging of the foils was carried out at the Natural History Museum. Craters were measured following the method of [6]; crater diameters were defined as the distance from top of the crater lip to top of the diametrically opposed crater lip. Two measurements were made for each crater to minimise error.

Results:

Table 1: Measured projectile and crater diameters, mean crater diameter and impact speeds from LGG shots.

Mean projectile diameter, D_p, ±σ (μm)	Impact speed ±2% (km/sec)	No. of craters measured	Mean crater diameter, D_c, ±σ (μm)
10.0 ± 1.45	6.12	34	26.78±4.30
7.04 ± 0.71	6.27	28	20.36±4.74
4.80 ± 0.48	6.04	108	11.39±1.90
1.94 ± 0.16	6.22	103	3.00±0.30
0.93 ± 0.03	6.12	49	1.64±0.23
0.47 ± 0.01	6.13	3†	0.65±0.10

†Due to their small size, it was very difficult to ascertain that all craters made in this shot arose from silica impactors and not by contaminating LGG debris or fragments of shattered sodalime glass beads used to entrain the particles in the shot. The three craters measured here were confirmed as silica impactors by SEM-EDX analyses.

Density scaling: To normalise the new data (ρ_{silica} =2.2 g cm^{-3} [10]) to the same projectile density as the existing calibration (ρ_{soda} =2.4 g cm^{-3}) the crater diameters, D_c, data were scaled using experimental results given in Fig. 4 of. [9]. i.e.:

$$D_c/D_p = 1.9114 \ln(\text{proj. density g cm}^{-3}) + 2.8995$$

Thus we multiply the measured crater diameters in Table 1 by a factor of 1.038. Fig. 1 shows the projectile diameter vs. crater diameter after density scaling of the silica projectiles.

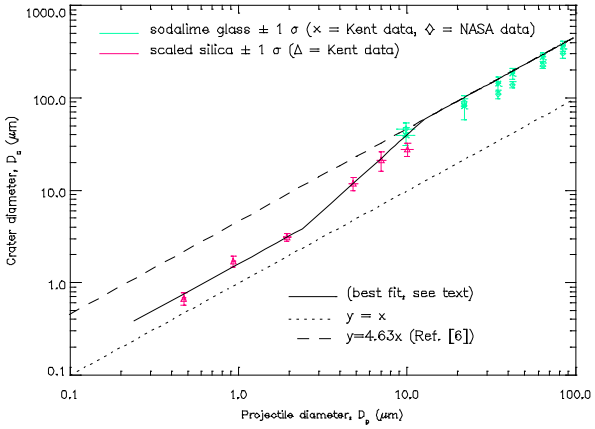

Fig.1: Sub 10-micron crater diameter vs. silica projectile diameter (density-scaled)

As can be seen in Fig. 1, at projectile diameters less than 10 μm, the ratio D_c/D_p is no longer a fixed constant. Investigations are underway as to the cause of this phenomenon, but it is speculated that it is due to the the pressure and temp. of the Al. during impact falling below that required for melting and/or a 'skin effect' caused by the work hardenening of the surface of the Al foil during its production. The solid line in Fig. 1 is a spline fit given by the following functions:

For $D_p < 2.4$ μm:

$$D_c = (1.60 \pm 0.17)\, D_p$$

For $2.4 < D_p < 12.7$ μm:

$$D_c = (0.91 \pm 1.89) D_p^{(1.64 \pm 0.92)}$$

For $D_p > 12.7$ μm:

$$D_c = (4.62 \pm 0.14)\, D_p$$

Discussion: Fig. 2 shows how these new results modify the cumulative size distribution of Stardust impactors as given in [4] for the Al foil crater data: power law fits to both the original data from [4] and the rescaled data are shown The index of the cumulative size distribution changes from its previous value of -1.72 [4] to -1.89, indicating that a larger mass fraction is contained within smaller projectiles than initially assumed. For craters with a diameter of less than 1 micron, the impactor mass increases by a factor of 20.

We finally take the rescaled data and plot it in Fig 3, along with other Stardust dust flux distribution data sets (i.e. including aerogel results, DFMI and CIDA) originally presented as Fig. 4 in [4].

Conclusions: New experimental data have enabled us to update the dust flux of comet 81P/Wild 2. The cumulative fluence data for projectiles of 5 μm dia. are now comparable to DMFI data, although there is a still a discrepancy with smaller projectiles. The results from 81P/Wild 2 have been compared to other comets [11], and the slope of the size distribution was intermediate between that for 26P/Grigg-Skjellerup (-0.93) [12] and that of 1P/Halley (-2.6±0.2) [13]. The updated slope found here (-1.89) is slightly closer than before to that of 1P/Halley but not sufficiently to classify it as the same type. This new work with small impactors also has implications for on-going investigations of the morphologies of small, complex craters seen on Stardust foils. To extend and refine the work further, smaller (0.1μm dia.) silica spheres have also been obtained and fired at foil, as well as repeat shots at larger sizes to improve measurement statistics. Their analysis is underway and this will extend the size of the crater calibration to cover the entire range of Stardust data.

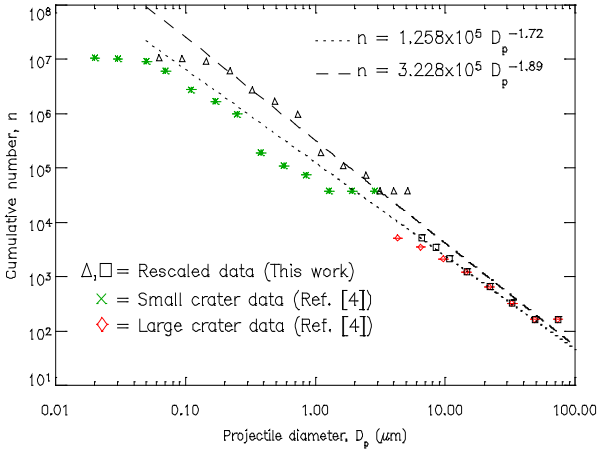

Fig. 2: Cumulative particle size distribution obtained from craters in Al foil on the Stardust spacecraft.

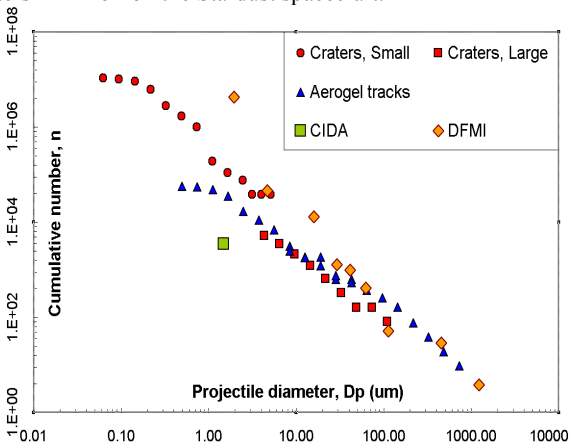

Fig 3: Updated Stardust dust fluence curve for 81P/Wild2

References: [1] Hanner M.S. and Bradley J.P. (2004) In *Comets II*, 555-564. [2] McDonnell J.A.M. et al. (1986) *Nature,* 321, 338-341. [3] Brownlee D.E. et al (2006) *Science, 314,* 1711–1716. [4] Hörz F. et al. (2006) *Science, 314,* 1716-1719. [5] Tuzzolino A.J. et al. (2004) *Science, 304,* 1776-1780. [6] Kearsley A.T. et al. (2006) *MAPS., 41,* 167-180. [7] Kearsley A.T. et al. (2008) *Int. J. Impact Eng., 35,* 1616-1624. [8] Burchell M.J. et al. (1999) *Meas. Sci. Tech., 10,* 41-50. [9] Kearsley A.T. et al. (2007) *MAPS., 42,* 191–210. [10] Rideal G., Whitehouse Scientific, private comm. (2008). [11] Burchell M.J. et al. (2008) *MAPS.,* 43, 23–40. [12] McDonnell J. A. M. et al (2001) *Comets in the post Halley era.* (Vol. 2, 1043-1073). [13] Fulle M. et al (2000) *Ap. J.*, *119,* 1968-1977.